

## A novel parallel chaotic system with greatly improved Lyapunov exponent and chaotic range

Minghao Zhu\* and Chunhua Wang<sup>†</sup>

*School of Information Science and Engineering,  
Hunan University, Changsha 410082, P. R. China*

\*zhuminghao0412@163.com

<sup>†</sup>wch1227164@hnu.edu.cn

Received 7 November 2019

Revised 25 December 2019

Accepted 2 January 2020

Published 17 March 2020

Lyapunov exponent (LE), chaotic range and complexity are the key considerations of a discrete chaotic system. A dynamic chaotic system with larger LE and wider parameter space will result in better statistical performance that can be used to generate pseudo random sequences and applied to encryption fields. At the same time, the combination of simple chaotic maps can generate more excellent chaotic behavior. This paper proposes a newly combined chaotic system called Parallel Chaotic System (PCS). Multiple simple chaotic maps are paralleled to construct the novel system. In this system, LE and chaotic range can be improved as much as possible by setting additional parameters. Compared with the existing models made up of same seed maps, PCS is able to get better chaotic behavior by means of a simple structure at the same time. Performance evaluation emphasizes that the chaotic maps generated by PCS are more unpredictable with better complexity.

*Keywords:* Parallel chaotic system (PCS); combined chaotic system; chaotic maps; Lyapunov exponent; chaotic ranges.

PACS number: 05.45.Ac

### 1. Introduction

Chaotic behavior, as a novel nonlinear dynamic behavior, was first discovered in meteorology as the butterfly effect.<sup>1</sup> It means that small changes in initial conditions can drive long-term and large chain reactions of the entire system. The basic characteristic of a chaotic system is its extreme sensitivity to initial value. The trajectories generated by two nearly identical initial values are separated exponentially as time goes on, and Lyapunov exponent (LE) is a quantitative description of

<sup>†</sup>Corresponding author.

this phenomenon.<sup>2</sup> Therefore, the increase of LE means the chaotic system is more sensitive to the initial value with better dynamic characteristics. The chaotic range is another important characteristic. The narrow chaotic range represents that the chaos can easily disappear after interference. In other words, wider chaotic range can acquire higher security. Chaotic motion also has other characteristics, such as boundedness, ergodicity and unpredictability. Because of these unique properties, chaos has been applied in many aspects especially in chaotic secure communication,<sup>2,3</sup> chaotic image encryption,<sup>4,5</sup> pseudo-random number generator<sup>6,7</sup> and other security fields.

The current chaotic systems can be divided into two types: (1) one-dimension (1D) and (2) high-dimension (HD). Compared with 1D chaotic maps, HD chaotic maps, like Lorenz chaotic system,<sup>8,9</sup> strange attractor of chaos<sup>10–17</sup> and some discrete hyperchaotic systems,<sup>18–20</sup> usually have a higher LE, and their nonlinear behavior is more complex and unpredictable, but they have higher costs in computation and more difficulties in hardware implementation. Simultaneously, the simple chaotic maps, like Logistic map, Sine map and Gauss map, have lower costs in computation and relatively simpler hardware circuit structure. Therefore, they can be easily realized in chaos-based applications. However, they have several security weaknesses: (1) their chaotic ranges are limited. (2) their LEs are usually small. (3) their outputs are easy to be predicted with low computation costs.

In order to overcome these defects of 1D chaotic maps, it is very necessary to design a map with better chaotic performance. Recently, some efforts have been made by combining them together. In general, there are four kinds of models of chaotic systems. The first kind of model is cascade chaotic system<sup>21</sup> which is essentially a composite function map. Its LE is the sum of inner and outer seed maps. Only when the iterative function is matched can it have a good chaotic performance. Its chaotic range is expanded compared with its seed maps but the improvement of LE is limited. Similarly, a robust chaos<sup>22</sup> was obtained by the sinusoidal transformation after the combination of two seed maps.<sup>23</sup> Its LE is the sum of the two seed maps and a Sine map. The second kind of model is parameter-modulated chaotic system<sup>24</sup> where a seed map is used to dynamically modulate another map. The linear transformation ensures that the iterative value of the controlling map is transformed to the chaotic range of the modulated map. It greatly expands the chaotic range and improves the initial value sensitivity of the system. Only the modulated seed map as the iterative function of the system, it does not essentially improve LE. The third kind of model is fusion model.<sup>25</sup> According to the threshold of the controller, one of the seed maps is selected for each iteration but it cannot fundamentally improve LE either. The last model is modulo operation.<sup>26</sup> Through a modulo operation, the output of the two seed maps is controlled in a certain area. However, its LE fails to improve a lot and the hardware implementation of modulo operation is complex. In order to obtain a much more complicated chaotic behavior, Refs. 27 and 28 came up with an idea of multilayer cascade, multilayer modulation and combination of

basic models. It may have a higher LE and a wider chaotic range but it gains better chaotic performance at the expense of harder hardware implementation. In short, compared with their corresponding seed maps, the maps generated by the above chaotic systems may have wider chaotic ranges. However, their LEs are still too small and their systems are not able to improve the LE as much as possible. In addition, their chaotic ranges are not wide enough.

Generally speaking, wide chaotic range, large LE and simple structure of hardware implementations are all important aspects to be considered in designing a chaotic system. Obviously, the above systems do not meet these design requirements. The previous contributions to the combined chaotic systems have two shortcomings: (1) chaotic behavior is limited and (2) better chaotic behavior is obtained at the expense of hardware implementation. However, we find a more ingenious method to overcome this deficiency by designing a Parallel Chaotic System (PCS). Compared with the published combined models composed of consistent seed maps, PCS can apparently improve LE as much as possible and obtain wider chaotic range through a relatively simple hardware structure. The iterative function of any 1D chaotic map that is always bounded can be used as a seed map of PCS. Setting different controlled parameters, using different seed maps, or exchanging seed maps can produce a series of chaotic systems with better chaotic performance. Here, we mainly compare with cascade chaotic system, fusion model, parameter-modulated chaotic system and modulo operation model.

The rest of the paper is organized as follows. Section 2 will illustrate the framework of PCS and provide relevant proof. Section 3 will briefly reviews two traditional chaotic maps. Section 4 gives three specific examples. Section 5 will justify the chaotic performance of PCS, including iteration function diagram, LE and Spectral entropy (SE). Finally, conclusions are summarized in Sec. 6.

## 2. Proposed Parallel Chaotic System and Analysis

The PCS is shown in Fig. 1 where  $f_1, f_2, \dots, f_k$  denote seed map functions and  $u_i (i \in [1, k]), c_i (i \in [1, k])$  are all parameters. Moreover,  $u_i$  is inherent to the system while  $c_i$  (we call it the controlled parameters) can be freely set by the user. The inputs are expanded by  $c_i$  times, respectively, for each seed map functions and we consider the sum of the all seed maps as output of the system so that each iteration can be carried out. Clearly, it can be seen that the new system consists of several seed maps in parallel.

From Fig. 1, the mathematical model can be obtained by

$$x_{n+1} = P(x_n) = \sum_{i=0}^{k-1} f_i(u_i, c_i x_n), \quad (1)$$

where  $P(x_n)$  denotes total map function of PCS.

As we all know, the LE indicates the numerical characteristics of the average exponential divergence rate of adjacent trajectories in phase space. It is one of the

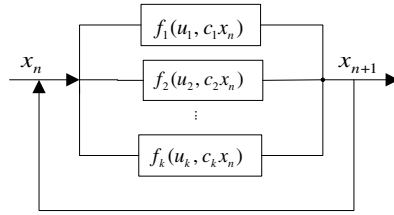


Fig. 1. Structure of PCS.

features used to identify chaotic motion and is an important indicator for chaotic dynamic performance. For a differentiable first-order difference equation  $x_{i+1} = f(x_i)$ , its LE can be defined by

$$LE_{f(x)} = \lim_{n \rightarrow \infty} \frac{1}{n} \sum_{i=0}^{n-1} \ln |f'(x_i)|. \tag{2}$$

According to the iterative equation of PCS, its LE can be obtained by

$$\begin{aligned} LE_{P(x)} &= \lim_{n \rightarrow \infty} \frac{1}{n} \sum_{i=0}^{n-1} \ln |P'(x_i)| \\ &= \lim_{n \rightarrow \infty} \frac{1}{n} \sum_{i=0}^{n-1} \ln \left| \left( \sum_{j=0}^{k-1} f_j(c_j x_i) \right)' \right| \\ &= \lim_{n \rightarrow \infty} \frac{1}{n} \sum_{i=0}^{n-1} \sum_{j=0}^{k-1} \ln |c_j f'_j(c_j x_i)| \\ &= \lim_{n \rightarrow \infty} \frac{1}{n} \sum_{i=0}^{n-1} \sum_{j=0}^{k-1} \ln |f'_j(c_j x_i)| + \sum_{j=0}^{k-1} \ln |c_j| \\ &= \sum_{j=0}^{k-1} LE_{f_j} + \sum_{j=0}^{k-1} \ln |c_j|. \end{aligned} \tag{3}$$

A positive LE means that the phase volume of the system is expanding and folding in this direction, and the adjacent orbits in the attractor are becoming more and more irrelevant, making the initial state unpredictable for the long of any uncertain system. That is chaotic behavior. Therefore, PCS is chaotic when  $LE_{P(x)} > 0$ . For the convenience of analysis, we assume  $c_j > 0$ . It is obvious that the LE of the original system  $f_i (i \in [1, k])$  can acquire gains to a certain extent when

$$\prod_{j=0}^{k-1} c_j > 1. \tag{4}$$

In theory, LE of PCS can be very large.

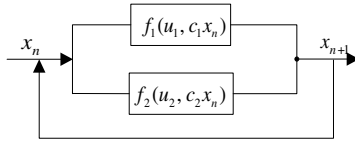


Fig. 2. Structure of PCS when  $k = 2$ .

PCS offers users a great deal of flexibility to choose seed maps to generate chaotic systems with higher LE and wider chaotic range. In order to facilitate further research, we just consider  $k = 1$ ,  $k = 2$  and  $k = 3$ .

- (1) When  $k = 1$ , PCS has only one seed map. In this case, the user’s utilization of the seed map is limited, but better chaotic behavior can still be obtained compared to the original seed map.
- (2) When  $k = 2$ , the corresponding block diagram of PCS is shown in Fig. 2.

In this case, PCS can be defined as

$$x_{n+1} = P(x_n) = f_1(u_1, c_1 x_n) + f_2(u_2, c_2 x_n), \tag{5}$$

where  $f_1$  and  $f_2$  may be same, or different. At this time, if  $f_1$  and  $f_2$  are exchanged each other, they are two completely different chaotic systems shown in Eq. (6),

$$x_{n+1} = P(x_n) = f_2(u_2, c_1 x_n) + f_1(u_1, c_2 x_n). \tag{6}$$

- (3) When  $k = 3$ , our main purpose is to verify the influence of the increase of  $k$  on the entire chaotic system based on the original map. The relevant system are shown in Fig. 3. In this case we can find the superiority when  $k$  increases, but the structure of system will be more complicated.

In short, PCS can produce a series of new maps with higher LE and wider chaotic range by selecting different seed map or exchanging the positions of seed map. By setting  $c_i$ , our system can apparently improve its LE. This is going to be validated in Sec. 4.

Moreover, when the structure of PCS is further extended, it offers users even more flexibility of selecting seed maps. The resulting chaotic maps have much more complicated chaotic behaviors and more parameter settings, and thus they may have

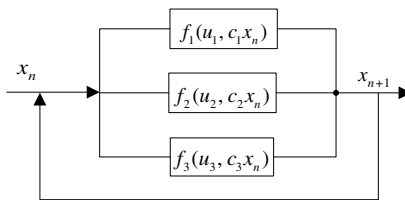


Fig. 3. Structure of PCS when  $k = 3$ .

much better chaotic performance and generate more random and unpredictable output sequences. Once a chaotic map generated by PCS is expanded, its LE will inevitably increase. On the other hand, however, multilayer parallel connections may result in many side effects including significant time delay, difficulty in hardware implementation, and complexity of performance analysis.

### 3. 1D Seed Maps

In this section, we will focus on two classical maps that will be considered as the seed map of the PCS to produce a series of new maps.

#### 3.1. Sine map (SM)

It is well-known that sine functions are always bounded, which satisfy the condition of the PCS. SM is defined as

$$x_{n+1} = S(x_n) = u \sin(\pi x_n), \quad u \in [0, 1], \quad (7)$$

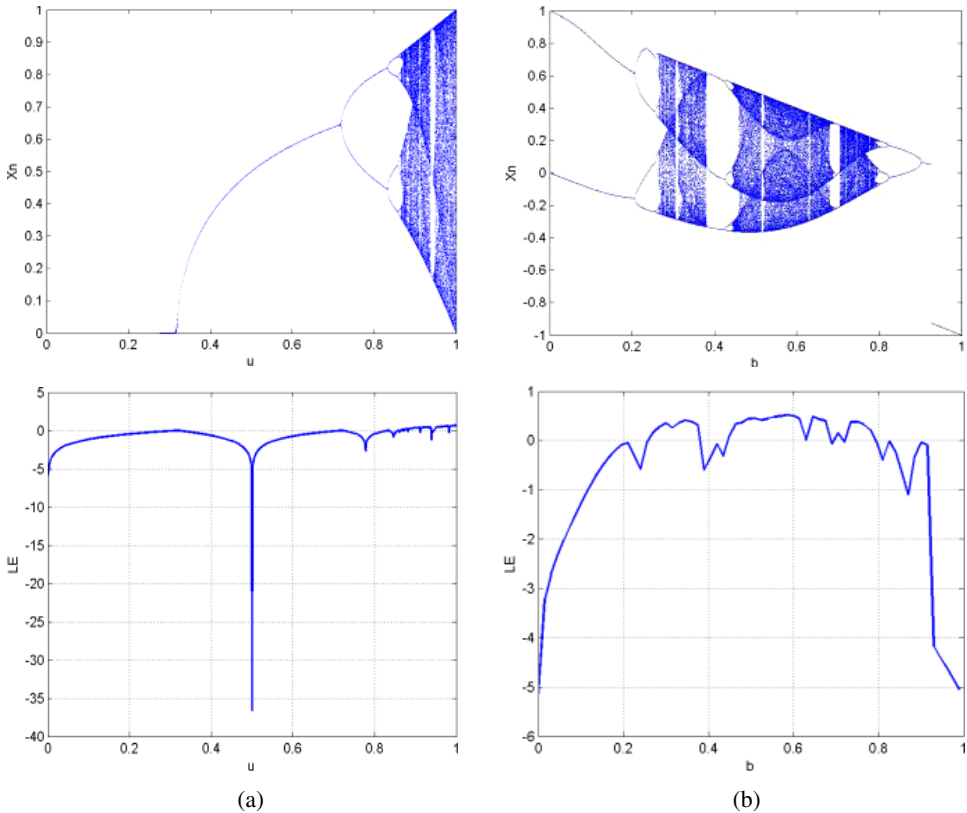


Fig. 4. (Color online) The bifurcation diagrams and corresponding LEs of the (a) SM and (b) GM.

where  $S(x_n)$  is SM function,  $u \in [0, 1]$  denotes inherent parameter. Its bifurcation diagram and its corresponding LE are shown in Fig. 4(a). SM has chaotic behavior when the parameter  $u$  is around  $[0.867, 1]$ . In addition, the closer the  $u$  is to 1, the better chaotic behavior is.

### 3.2. Gauss map (GM)

GM comes from the Gaussian function named after Carl Friedrich Gauss. GM is defined as follows:

$$x_{n+1} = G(x_n) = e^{-ax_n^2} - b, \quad b \in [0, 1], \quad (8)$$

where  $G(x_n)$  is GM function,  $a \in [0, 8]$  and  $b \in [0, 1]$  are inherent parameters that control the width and height of the Gauss curve, respectively.<sup>29</sup> It can be concluded from (8) that the GM is still bounded and  $x$  is in the range of  $[-1, 1]$ . The bifurcation diagram and the corresponding LE are given in Fig. 4(b) when  $a = 8$ .

## 4. Examples of Parallel Chaotic System

Using different 1D chaotic maps as seed maps, PCS is able to generate a large number of new maps. This section provides three examples to show the availability of the PCS.

### 4.1. Enhanced-sine map (ESM)

When the PCS has only one seed map ( $k = 1$ ), the example is

$$x_{n+1} = u^* \sin(\pi^* c^* x_n), \quad u \in [0, 1], \quad (9)$$

where  $u$  is an inherent parameter and  $c$  is a controlled parameter.

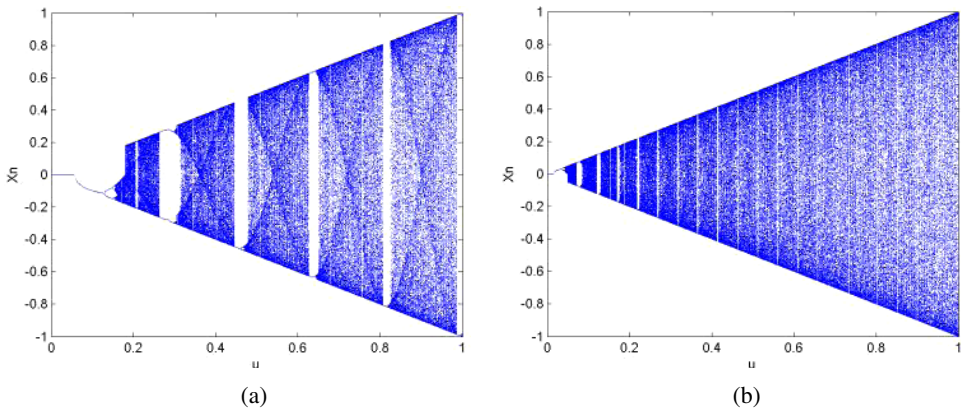


Fig. 5. (Color online) The bifurcation diagram of ESM when (a)  $c = 5.56$  and (b)  $c = 20.56$ .

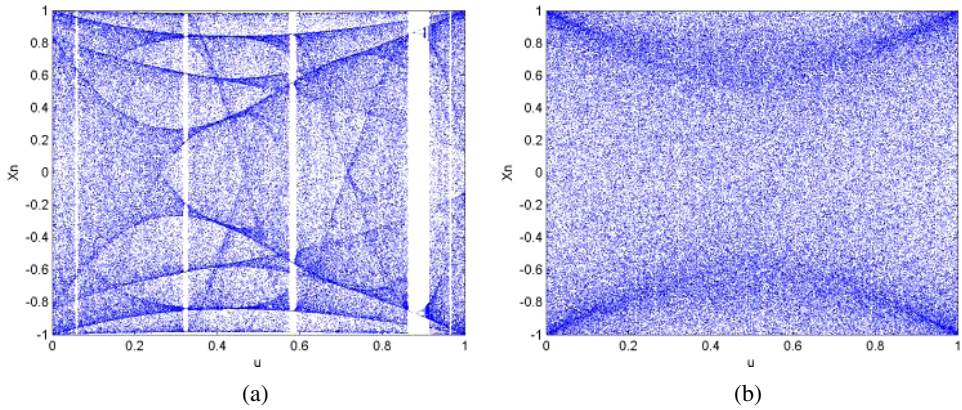


Fig. 6. (Color online) The bifurcation diagram of SSM when (a)  $c_1 = 2.96$ ,  $c_2 = 2.32$  and (b)  $c_1 = 50.96$ ,  $c_2 = 50.32$ .

We get its bifurcation diagram separately when  $c$  is 5.56 in Fig. 5(a) and 20.56 in Fig. 5(b). It is obvious that the chaotic range increases significantly as  $c$  becomes larger. This means that the controlled parameter  $c$  can enhance chaotic performance.

#### 4.2. Sine-sine map (SSM)

In Eq. (5), when  $f_1$  and  $f_2$  are the same ( $k = 2$ , both  $f_1$  and  $f_2$  are SM), the iteration of PCS is

$$x_{n+1} = u^* \sin(\pi^* c_1^* x_n) + (1 - u)^* \sin(\pi^* c_2^* x_n), \quad u \in [0, 1], \quad (10)$$

where  $u$  is an inherent parameter and  $c_i (i \in [1, 2])$  is a controlled parameter.

It is clear that  $x$  is still bounded. We can observe its bifurcation diagram when  $c_1 = 2.96$  and  $c_2 = 2.32$  in Fig. 6(a) and when  $c_1 = 50.96$  and  $c_2 = 50.32$  in Fig. 6(b). More worth mentioning is that Fig. 6(b) has no periodic window, in this way, chaotic map is generated in the whole region.<sup>30,31</sup> This is called as robust Sine-Sine Map (RSSM).

#### 4.3. Gauss-sine map (GSM) and sine-gauss map (SGM)

When  $f_1$  and  $f_2$  are different ( $k = 2$ ,  $f_1$  is a GM and  $f_2$  is a SM), we get Gauss-Sine Map (GSM). Its mathematical equation is shown in Eq. (11)

$$x_{n+1} = e^{-a^*(c_1^* x_n)^2} - u + (1 - u)^* \sin(\pi^* c_2^* x_n), \quad a = 8, \quad u \in [0, 1], \quad (11)$$

where  $u$  is an inherent parameter and  $c_i (i \in [1, 2])$  is a controlled parameter.

Mathematically, the result of the addition of bounded functions is still bounded and thus  $x$  is still always bounded. We set  $c_1 = 12.86$ ,  $c_2 = 5.56$  to obtain its bifurcation diagram shown in Fig. 7(a). Then, in Eq. (6), we simply exchange the



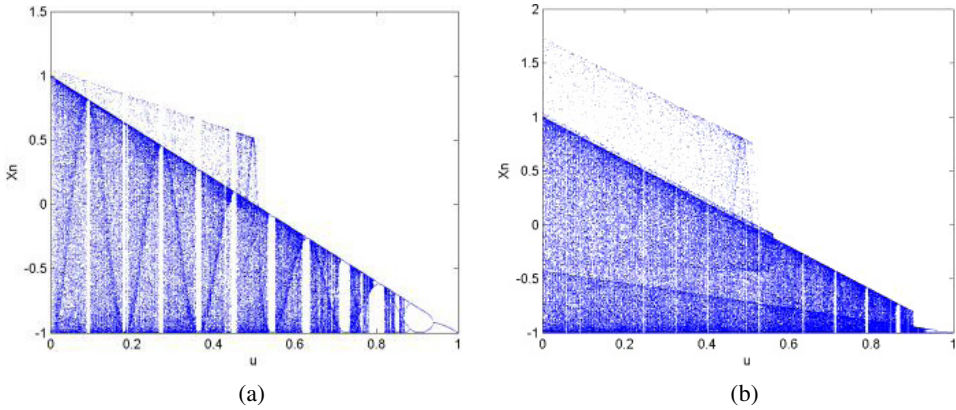


Fig. 7. (Color online) the bifurcation diagram of GSM when (a)  $c_1 = 12.86$ ,  $c_2 = 5.56$  and SGM when and (b)  $c_1 = 5.56$ ,  $c_2 = 12.86$ .

two seed maps of GSM to get a new map called Sine-Gauss Map (SGM). Its iterative equation is shown in Eq. (12) and its bifurcation diagram is shown in Fig. 7(b).

$$x_{n+1} = e^{-a^*(c_2^*x_n)^2} - u + (1 - u)^* \sin(\pi^*c_1^*x_n), \quad a = 8, \quad u \in [0, 1]. \quad (12)$$

Similarly,  $u$  is an inherent parameter and  $c_i (i \in [1, 2])$  is a controlled parameter.

From Fig. 7 we can observe that exchanging the position of the seed map will have totally different chaotic behavior. This is consistent with our previous inference in Sec. 2.

In addition, in order to verify the effect of extended PCS ( $k = 3$ ) on chaotic performance, we expand on GSM and SGM. We give the relevant mathematical definition of new chaotic maps.

(1) When expanding on GSM, the new map is

$$x_{n+1} = e^{-a^*(c_1^*x_n)^2} - u + (1 - u)^* \sin(\pi^*c_2^*x_n) + u^* \sin(\pi^*c_3^*x_n), \quad a = 8, \quad u \in [0, 1], \quad (13)$$

where  $c_i (i \in [1, 3])$  are all controlled parameters ( $c_1 = 12.86$ ,  $c_2 = 5.56$ ,  $c_3 = 12.23$ ) and  $u$  is an inherent parameter. We get the bifurcation diagram of extended GSM in Fig. 8(a).

(2) When expanding on SGM, we get approximately the same map as the extended GSM. Its iterative equation is

$$x_{n+1} = e^{-a^*(c_2^*x_n)^2} - u + (1 - u)^* \sin(\pi^*c_1^*x_n) + u^* \sin(\pi^*c_3^*x_n), \quad a = 8, \quad u \in [0, 1]. \quad (14)$$

We get the bifurcation diagram of extended SGM in Fig. 8(b).

From Figs. 7 and 8, we can find that Figs. 7(a) and 7(b) has many obvious periodic windows whereby specific values of  $u$  will cause the chaotic map to behave

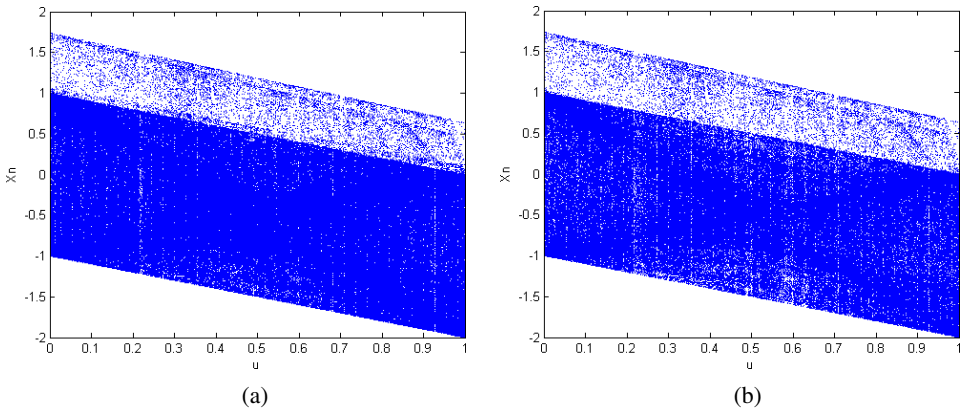


Fig. 8. (Color online) The bifurcation diagram of extended GSM when (a)  $c_1 = 12.86$ ,  $c_2 = 5.56$ ,  $c_3 = 12.23$  and extended SGM when and (b)  $c_1 = 5.56$ ,  $c_2 = 12.86$ ,  $c_3 = 12.23$ .

in a periodic manner. However, there are small periodic regions in Figs. 8(a) and 8(b). In addition, the bifurcation diagram of extended GSM and extended SGM can cover all possible points in the phase space under the same chaotic range, which will lead to a better ergodicity. This means that the extended GSM and extended SGM have better chaotic performances.

## 5. Performance Evaluations and Comparisons

In order to further prove the chaotic performance and further highlight the advantages of PCS, we first perform iteration function diagram and then compare the new chaotic maps with their seed maps and other chaotic systems by LE and SE in this section.

### 5.1. Iteration function diagram

For an iterative dynamical system like  $x_{n+1} = f(x_n)$ , the iteration function diagram describes the output  $x_{n+1}$  along with the input  $x_n$ .

Obviously, the iteration function diagram of new maps generated by PCS in Fig. 9 have more complex patterns than their seed maps. This is because the controlled parameters are added and their outputs are combinations of chaotic orbits of seed maps. These new maps are so difficult to predict that they are more secure and more suitable for security applications.

### 5.2. LEs

A dynamic system with a positive LE is considered to have chaotic behavior, and a bigger LE means a better chaotic behavior. Clearly, the new maps generated by PCS is larger than its seed maps under the same chaotic range in Fig. 10. Simultaneously, if we increase controlled parameter, the LE corresponding to the new map will

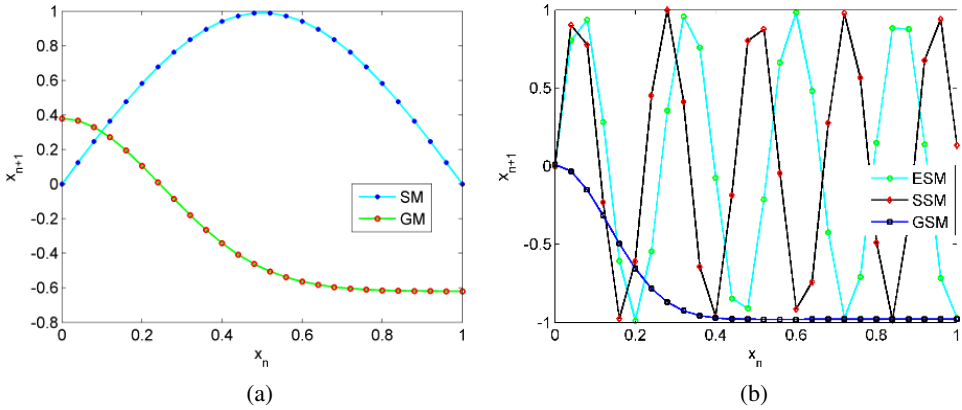


Fig. 9. (Color online) The iteration function diagram of (a) SM, GM and (b) ESM, SSM, GSM.

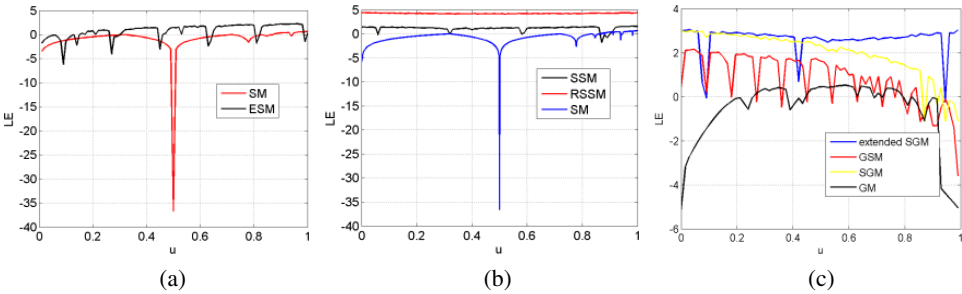


Fig. 10. (Color online) LE comparisons of (a) SM, ESM, (b) SSM, RSSM, SM and (c) extended SGM, GSM, SGM, GM.

also become larger. Although GSM and SGM have the same seed maps, they are completely different chaotic systems which coincides with the previous proof in Secs. 2 and 4.3. In addition, the expanded SGM has a higher LE.

Furthermore, to facilitate the observation of the superiority of our system over other systems including the aforementioned cascade chaotic system, fusion model, parameter-modulated chaotic system and modulo operation model, we list a Table 1. GM and SM are selected as seed maps for each system, respectively. we take  $u$ ,  $a$ , or  $b$  as the inherent parameters of each system. As a result, under the condition of same seed maps, our system is able to have larger LE and wider chaotic ranges compared with other combined systems.

When a chaotic map generated by PCS expands, his LE will inevitably become larger. In order to verify that its LE changes with the number of parallel layers  $k$ , we take the Sine map as a seed map (refer to Eqs. (9) and (10)) and choose significant controlled parameters, respectively. Table 2 means that when a new map is further expanded, its LE will certainly increase.

Table 1. The comparisons of the largest LE and chaotic range.

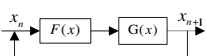
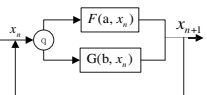
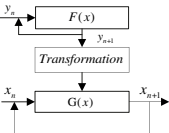
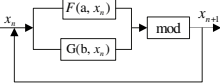
Systems	Definition of maps	LE	Chaotic range in [0, 1]
Cascade: 	$x_{n+1} = u^* \sin(\pi^*(e^{-a^*} x_n^2 - b))$ where $a = 8, b = 0.62$ .	0.554	[0.328, 0.456]
Fusion: 	$x_{n+1} = \begin{cases} u^* \sin(\pi^* x_n), & y_n < 0.5, \\ e^{-a^*} x_n^2 - u, & y_n \geq 0.5, \end{cases}$ where $y_{n+1} = 4^* u^* y_n^*(1 - y_n), a = 8$ .	0.504	[0.499, 0.631] ∪ [0.952, 0.961]
Modulation: 	$x_{n+1} = (1 - 0.13^* y_n)^* \sin(\pi^* x_n)$ where $y_{n+1} = e^{-a^*} y_n^2 - b, a = 8$ .	0.651	[0.049, 1]
Modulo operation: 	$x_{n+1} = (e^{-a^*} x_n^2 - u + (1 - u)^* \sin(\pi^* x_n)) \bmod 1$ where $a = 8$ .	0.761	[0.112, 0.324] ∪ [0.613, 0.757]
Our work (SGM)	Eq. (11) where $a = 8, c_1 = 5.56, c_2 = 12.86$ .	2.995	[0, 0.935]
Our work (SGM)	Eq. (11) where $a = 8, c_1 = 125.56, c_2 = 150.86$ .	7.831	[0, 0.992]
Our work (extended SGM)	Eq. (13) where $a = 8, c_1 = 5.56, c_2 = 12.86, c_3 = 12.23$ .	3.054	[0, 1]

Table 2. LE of extended new map varies with  $k$ .

$k$	1	2	3	5	7
Controlled parameters $c_i (i \in [1, k])$	$c_1 = 5.56$	$c_1 = 5.56$ $c_2 = 12.86$	$c_1 = 5.56$ $c_2 = 12.86$ $c_3 = 20.32$	$c_1 = 5.56$ $c_2 = 12.86$ $c_3 = 20.32$ $c_4 = 34.56$ $c_5 = 46.86$	$c_1 = 5.56$ $c_2 = 12.86$ $c_3 = 20.32$ $c_4 = 34.56$ $c_5 = 46.86$ $c_6 = 52.32$ $c_7 = 65.56$
LE	2.263	3.029	3.545	4.322	6.827

### 5.3. Complexity analysis

The complexity of a chaotic system refers to the use of related algorithms to measure the extent of its chaotic sequence approaching random sequence. The greater the complexity is, the closer the sequence is to the random sequence and the higher the corresponding security is. Here, we use a SE, an algorithm of structural complexity,

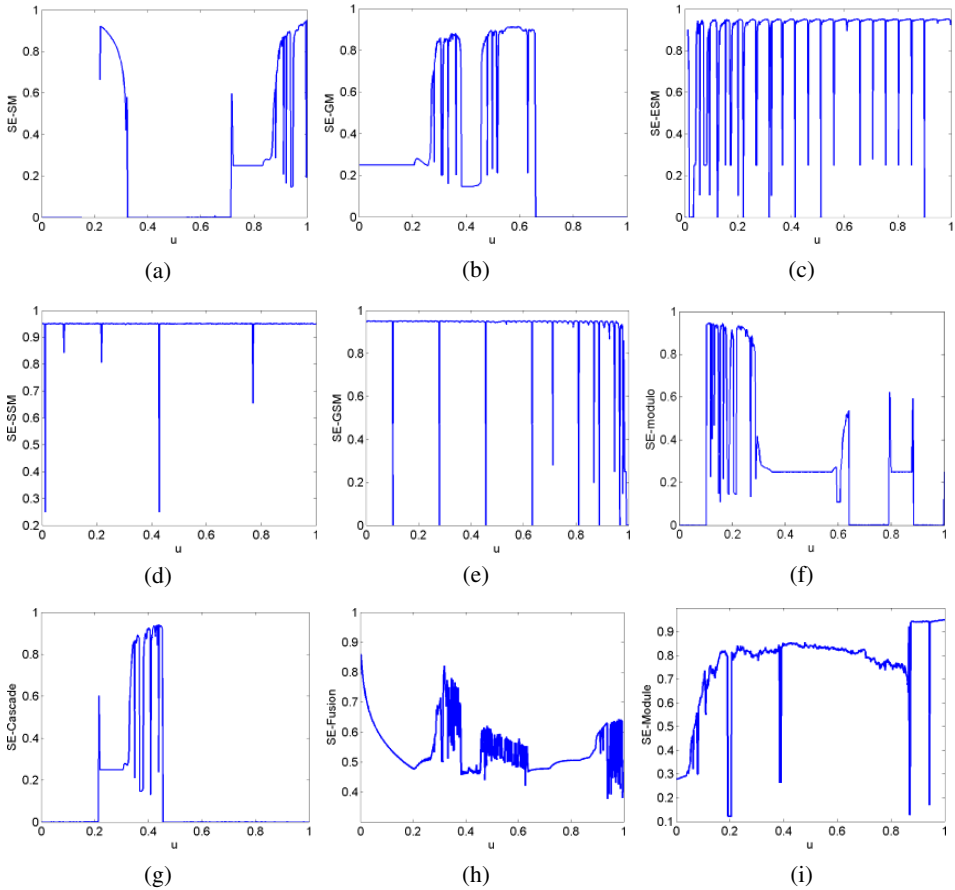


Fig. 11. (Color online) The SE of (a) SM (b) GM, (c) ESM, (d) SSM, (e) GSM, (f) modulo, (g) cascade, (h) fusion and (i) modulation.

based on Fourier transform for complexity analysis.<sup>32</sup> A larger SE means that the corresponding dynamic system is more complex.

Figure 11 simulates the situation when the complexity of each map in Table 1 changes with the parameters. It is obvious that the SE increases obviously under the corresponding chaotic range, but the SE is very small even close to 0 in conditions of the periodic state. It is worth mentioning that the complexity of each new maps in Figs. 9(c)–9(e) is larger than 0.9 almost on the total parameter range. On the premise of parameter variation, the SE of our system can still remain a high level. In other words, our system has a better dynamic complexity and the new maps generated by PCS are closer to a random sequence.

## 6. Conclusions

In view of the defects of 1D simple chaotic maps, such as small LE and narrow chaotic range, this paper have proposed a novel PCS based on the existing combined

chaotic systems. Under the condition of same seed maps, our system has obvious advantages compared with the existing combined chaotic systems. PCS can improve LE as much as possible and the chaotic range is wider at the same time. Whats more significant is that we can get a better chaotic behavior through a simple structure. In addition, we have evaluated and further highlighted the advantages of our system through iteration function diagram, the comparisons of LE and SE in the end.

## Acknowledgments

This work was supported in part by the National Natural Science Foundation of China under Grant No. 61971185, the Major Research Plan of the National Natural Science Foundation of China under Grant No. 91964108 and the Open Fund Project of Key Laboratory in Hunan Universities under Grant No. 18K010.

## References

1. L. N. Edward and E. N. Lorenz, *Asia-Pac. J. Atmos. Sci.* **20**, 130 (1963).
2. P. Bryant, R. Brown and H. D. I. Abarbanel, *Phys. Rev. Lett.* **65**, 1523 (1990).
3. L. M. Pecora and T. L. Carroll, *Synchronization in Chaotic Systems, Controlling Chaos.* **6** 142 (1996).
4. Q. Yin and C. H. Wang, *Int. J. Bifurcation Chaos* **28**, 1850047 (2018).
5. G. F. Cheng, C. H. Wang and H. Chen, *Int. J. Bifurcation Chaos* **29**, 1950115 (2019).
6. A. Saito and A. Yamaguchi, *Chaos* **28**, 103122 (2017).
7. X. Wang and X. Qin, *Nonlinear Dyn.* **70**, 1589 (2012).
8. F. Q. Wang and C. X. Liu, *Int. J. Mod. Phys. B* **21**, 3053 (2007).
9. S. He, K. Sun and H. Wang, *Entropy* **17**, 8299 (2015).
10. L. Zhou and C. H. Wang, *Nonlinear Dyn.* **85**, 1 (2016).
11. C. H. Wang, X. Liu and X. Hu, *Chaos* **27**, 033114 (2017).
12. L. Zhou, C. H. Wang and L. L. Zhou. *Int. J. Circuit Theory Appl.* **46**, 84 (2018).
13. Q. L. Deng and C. H. Wang, *Chaos* **29**, 093112 (2019).
14. X. Zhang and C. H. Wang, *Int. J. Bifurcation Chaos* **29**, 1950117 (2019).
15. X. Zhang, C. H. Wang and W. Yao, *Nonlinear Dyn.* **97**, 2159 (2019).
16. X. Zhang and C. H. Wang, *IEEE Access* **7**, 16336 (2019).
17. P. Dong, K. Sun and O. A. Alamodi, *Int. J. Mod. Phys. B* **33**, 1950031 (2019).
18. W. Liu, K. Sun and S. He, *Nonlinear Dyn.* **89**, 2521 (2017).
19. M. Yu *et al.*, *Chaos Solitons Fractals* **106**, 107 (2018).
20. O. A. Alamod *et al.*, *Chin. Phys. B* **28**, 020503 (2019).
21. Y. Zhou, Z. Hua and C. M. Pun, *IEEE Trans. Cybern.* **45**, 2001 (2015).
22. M. Andrecut and M. K. Ali, *Int. J. Mod. Phys. B* **15**, 177 (2001).
23. Z. Hua, B. Zhou and Y. Zhou, *IEEE Trans. Ind. Electron.* **65**, 2557 (2018).
24. Z. Hua and Y. Zhou, *IEEE Trans. Cybern* **46**, 3330 (2015).
25. L. Bao, Y. Zhou and C. L. P. Chen, *Int. Conf. on System Science and Engineering*, 2012.
26. Y. Zhou, L. Bao and C. L. P. Chen, *Signal Process.* **97**, 172 (2014).
27. Z. Hua and Y. Zhou, *IEEE Trans. Circuits Syst. I Regul. Pap.* **65**, 235 (2018).
28. R. Lan, J. He and S. Wang, *Signal Process.* **147**, 133 (2018).
29. V. Patidar and K. K. Sud, *Commun. Nonlinear Sci. Numer. Simul.* **14**, 827 (2009).
30. E. Zeraoulia and J. C. Sprott, *Adv. Complex Syst.* **14**, 817 (2011).
31. M. Patra and S. Banerjee, *Chaos* **28**, 123101 (2018).
32. K. Sun, S. He and H. Yi, *Acta Phys. Sin.* **62**, 27 (2013).